Acta Cryst E CRYSTALLOGRAPHIC COMMUNICATIONS

ISSN 2056-9890

Received 25 March 2019
Accepted 31 March 2019

Edited by W. T. A. Harrison, University of Aberdeen, Scotland

‡ Additional correspondence author, e-mail: aasiri2@kau.edu.sa.

Keywords: crystal structure; pyrazolone; pyrazole; tautomer; Hirshfeld surface analysis.

CCDC reference: 1906841

Supporting information: this article has supporting information at journals.iucr.org/e

Co-crystallization of a neutral molecule and its zwitterionic tautomer: structure and Hirshfeld surface analysis of 5-methyl-4-(5-methyl-1*H*-pyrazol-3-yl)-2-phenyl-2,3-dihydro-1*H*-pyrazol-3-one 5-methyl-4-(5-methyl-1*H*-pyrazol-2-ium-3-yl)-3-oxo-2-phenyl-2,3-dihydro-1*H*-pyrazol-1-ide monohydrate

Abdullah M. Asiri,[a,b]‡ Khalid A. H. Alzahrani,[b] Hassan M. Faidallah,[b] Khalid A. Alamry,[b] Mukesh M. Jotani[c] and Edward R. T. Tiekink[d]*

[a]Center of Excellence for Advanced Materials Research, King Abdulaziz University, PO Box 80203, Jeddah 21589, Saudi Arabia, [b]Chemistry Department, Faculty of Science, King Abdulaziz University, PO Box 80203, Jeddah 21589, Saudi Arabia, [c]Department of Physics, Bhavan's Sheth R. A. College of Science, Ahmedabad, Gujarat 380001, India, and [d]Research Centre for Crystalline Materials, School of Science and Technology, Sunway University, 47500 Bandar Sunway, Selangor Darul Ehsan, Malaysia. *Correspondence e-mail: edwardt@sunway.edu.my

The title compound, $2C_{14}H_{14}N_4O\cdot H_2O$, comprises a neutral molecule containing a central pyrazol-3-one ring flanked by an N-bound phenyl group and a C-bound 5-methyl-1*H*-pyrazol-3-yl group (at positions adjacent to the carbonyl substituent), its zwitterionic tautomer, whereby the N-bound proton of the central ring is now resident on the pendant ring, and a water molecule of crystallization. Besides systematic variations in geometric parameters, the two independent organic molecules have broadly similar conformations, as seen in the dihedral angle between the five-membered rings [9.72 (9)° for the neutral molecule and 3.32 (9)° for the zwitterionic tautomer] and in the dihedral angles between the central and pendant five-membered rings [28.19 (8) and 20.96 (8)° (neutral molecule); 11.33 (9) and 11.81 (9)°]. In the crystal, pyrazolyl-N—H···O(carbonyl) and pyrazolium-N—H···N(pyrazolyl) hydrogen bonds between the independent organic molecules give rise to non-symmetric nine-membered {···HNNH···NC_3O} and {···HNN···HNC_3O} synthons, which differ in the positions of the N-bound H atoms. These aggregates are connected into a supramolecular layer in the *bc* plane by water-O—H···N(pyrazolide), water-O—H···O(carbonyl) and pyrazolyl-N—H···O(water) hydrogen bonding. The layers are linked into a three-dimensional architecture by methyl-C—H···π(phenyl) interactions. The different interactions, in particular the weaker contacts, formed by the organic molecules are clearly evident in the calculated Hirshfeld surfaces, and the calculated electrostatic potentials differentiate the tautomers.

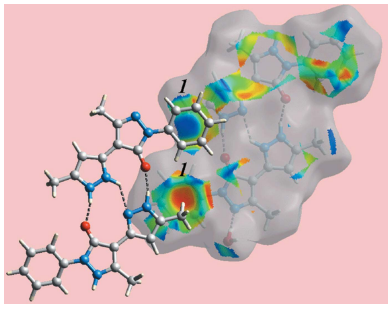

1. Chemical context

Molecules related to the title compound, *i.e.* containing a pyrazolone ring, are of particular interest owing to their pharmaceutical potential. Applications in this context include their possible utilization as cardiovascular drugs (Higashi *et al.*, 2006), as hypoglycemic agents (Das *et al.*, 2008) and as anti-inflammatory and analgesic agents (Badawey & El-Ashmawey, 1998). This class of compound has also been evaluated as anti-microbials (Sahu *et al.*, 2007) and display fungicidal activities (Singh & Singh, 1991). In the course of

studies in this area, the title compound, which has been synthesized previously (Kumar *et al.*, 1995), was characterized crystallographically on a crystal isolated from an ethanol solution and found to contain neutral and zwitterionic tautomers.

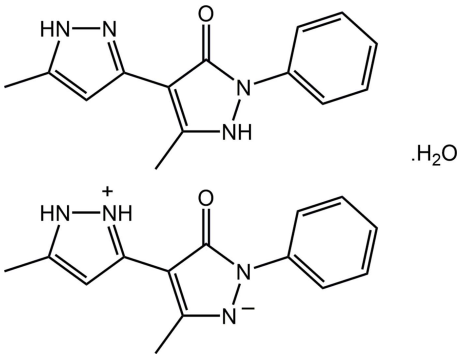

Tautomerism relates to a phenomenon whereby isomeric structures undergo inter-conversion by the migration of, typically, an atom, often a proton, or small group within the molecule. While different tautomers can co-exist in solution, in crystals usually only one form is found (Rubčić *et al.*, 2012). Notable examples of tautomers crystallizing in the same crystal begin with biologically relevant isocytosine (Sharma & McConnell, 1965) and the histidine residue in the structure of L-His-Gly hemihydrate (Steiner & Koellner, 1997). Such behaviour has also been observed, for example, in a synthetic compound, namely, *N*-(3-hydroxysalicylidene)-4-methoxyaniline (Pizzala *et al.*, 2000). Herein, the crystal and molecular structures of the title compound, (I), are described along with an analysis of the calculated Hirshfeld surfaces.

2. Structural commentary

The crystal of (I), Fig. 1, comprises a neutral molecule of 5-methyl-4-(5-methyl-1*H*-pyrazol-3-yl)-2-phenyl-2,3-dihydro-1*H*-pyrazol-3-one, its zwitterionic tautomer 5-methyl-4-(5-methyl-1*H*-pyrazol-2-ium-3-yl)-3-oxo-2-phenyl-2,3-dihydro-1*H*-pyrazol-1-ide and a molecule of water. Evidence of tautomerism is twofold. Firstly, in the nature of the hydrogen-bonding interactions operating in the crystal; see *Supramolecular features*. Secondly, in small but systematic variations in key geometric parameters, Table 1. Thus, the N5—N6 bond in the zwitterion is longer than the equivalent N1—N2 bond in the neutral species with a concomitant shortening of the C16—N6 and lengthening of the C16—C17 bonds with respect to the bonds in the neutral species. The most notable changes in angles relate to protonation/deprotonation. Thus, the angle at the protonated N2 atom is greater than the angle at the deprotonated N6, and the same is true for the angles subtended at the N7 and N3 atoms. Molecules in (I) may also exhibit rotational isomerism about the C3—C5 and C17—C19 bonds. In the present case, the carbonyl group is *syn* with the pendent ring imine-N atom in the neutral molecule and is designated the NH-*Z* form (Kumar *et al.*, 1995); the zwitterionic tautomer has a similar conformation.

The differences in geometric parameters characterizing the two independent organic molecules in (I) notwithstanding, the molecules present very similar conformations as highlighted in the overlay diagram, Fig. 2. Thus, the r.m.s. deviations of the

Table 1
Selected geometric parameters (Å, °) for (I).

Atoms	Parameter	Atoms	Parameter
C1—O1	1.266 (2)	C15—O2	1.263 (2)
N1—N2	1.376 (2)	N5—N6	1.401 (2)
C1—N1	1.389 (2)	C15—N5	1.396 (2)
C2—N2	1.338 (2)	C17—N6	1.329 (2)
C1—C3	1.429 (2)	C15—C17	1.416 (2)
C2—C3	1.391 (2)	C16—C17	1.405 (2)
N3—N4	1.364 (2)	N7—N8	1.349 (2)
C5—N3	1.346 (2)	C19—N7	1.349 (2)
C7—N4	1.338 (2)	C21—N8	1.337 (2)
C5—C6	1.414 (2)	C19—C20	1.404 (2)
C6—C7	1.375 (2)	C20—C21	1.389 (2)
N2—N1—C1	109.07 (13)	C15—N5—N6	111.51 (13)
N2—N1—C9	121.16 (14)	N6—N5—C23	119.25 (14)
C1—N1—C9	129.62 (14)	C15—N5—C23	128.95 (15)
N1—N2—C2	108.78 (14)	N5—N6—C16	105.37 (13)
N4—N3—C5	103.94 (14)	N8—N7—C19	110.58 (14)
N3—N4—C7	113.60 (14)	N7—N8—C21	108.36 (14)

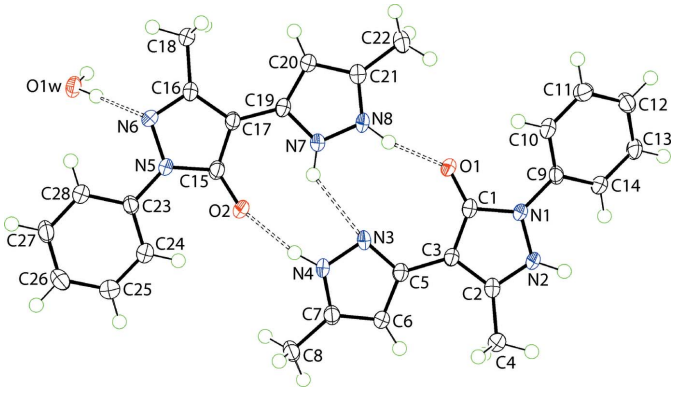

Figure 1
The molecular structures of the constituents of (I), showing displacement ellipsoids at the 70% probability level. The pyrazolyl-N4, N8—H···O2, O1(carbonyl), pyrazolium-N7—H···N3(pyrazolyl) and water-O—H···N6(pyrazolium) hydrogen bonds are shown as dashed lines. Note the non-symmetric nine-membered {···HNNH···NC$_3$O} and {···HNN···HNC$_3$O} synthons formed between the neutral and tautomeric molecules.

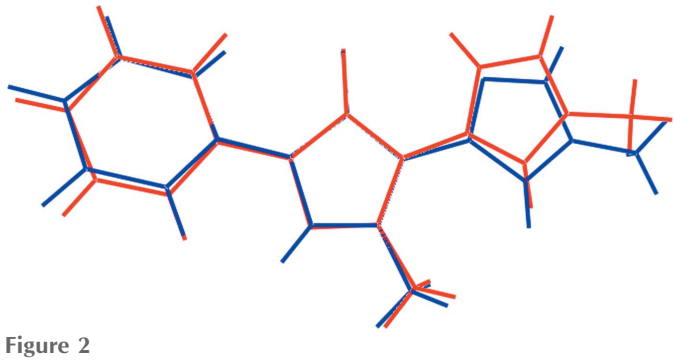

Figure 2
Overlay diagram of the two organic molecules in (I): neutral molecule (blue image) and zwitterion (red). The molecules have been overlapped so that the five-membered rings are coincident.

Table 2
Hydrogen-bond geometry (Å, °).

*Cg*1 is the centroid of the (C23–C28) ring.

D—H···*A*	*D*—H	H···*A*	*D*···*A*	*D*—H···*A*
N2—H2*N*···O1*W*^{i}	0.90 (1)	1.79 (1)	2.673 (2)	168 (2)
N4—H4*N*···O2	0.88 (1)	1.90 (1)	2.764 (2)	168 (2)
N7—H7*N*···N3	0.89 (1)	2.28 (2)	2.970 (2)	134 (1)
N8—H8*N*···O1	0.90 (1)	1.79 (1)	2.664 (2)	166 (2)
O1*W*—H1*W*···O1^{ii}	0.85 (2)	1.92 (2)	2.7641 (17)	172 (2)
O1*W*—H2*W*···N6	0.86 (2)	1.94 (2)	2.7979 (19)	178 (2)
C8—H8*A*···*Cg*1^{iii}	0.98	2.71	3.492 (2)	137
C8—H8*B*···*Cg*1^{iv}	0.98	2.89	3.755 (2)	148

Symmetry codes: (i) $x, -y+\frac{1}{2}, z+\frac{1}{2}$; (ii) $-x+1, -y+1, -z+1$; (iii) $-x+2, -y+1, -z+1$; (iv) $-x+2, -y, -z+1$.

fitted atoms of the N1, N3, N5 and N7 rings are 0.019, 0.003, 0.006 and 0.006, respectively. The dihedral angle between the N1 and N3 rings is 9.72 (9)°, and that between each of these and the appended phenyl ring are 28.19 (8) and 20.96 (8)°. The comparable values for the zwitterionic tautomer are 3.32 (9), 11.33 (9) and 11.81 (9)°, respectively, indicating that this molecule is closer to planar, as vindicated by the difference in the N2—N1—C9—C14 and N6—N5—C23—C28 torsion angles of 26.2 (2) and −7.4 (2)°, respectively.

3. Supramolecular features

The molecular packing of (I) features substantial conventional hydrogen-bonding interactions and the description of these can be conveniently divided by discussing interactions without the involvement of the water molecule of crystallization and then considering the role of the water molecule. Table 2 lists the geometric parameters of the specific intermolecular interactions in the crystal of (I). There are three hydrogen bonds formed between the two organic molecules comprising the asymmetric unit and these involve the three outer-ring amine-H atoms as donors and a ring-N and the two carbonyl-O atoms as acceptors. The resulting pyrazolyl-N4, N8—H···O1, O2(carbonyl) and pyrazolium-N7—H···N3(pyrazolyrazolyl) hydrogen bonds give rise to non-symmetric nine-membered {···HNNH···NC$_3$O} and {···HNN···HNC$_3$O} synthons, differing only in the relative placement of one of the ring-N-bound H atoms, Fig. 1. The two-molecule aggregates are assembled into a supramolecular layer in the *bc* plane by hydrogen bonding involving the water molecule, which functions as a donor to the pyrazolide-N6 and carbonyl-O1 atoms and as an acceptor from a pyrazolyl-N2 atom, Fig. 3*a*. Further consolidation of the layers is provided by π–π interactions with the shortest of these involving the N1-pyrazolyl and phenyl(C9–C14)^{i} rings [inter-centroid separation = 3.5810 (9) Å, inter-planar angle = 6.29 (8)° for symmetry operation: (i) $1-x, \frac{1}{2}+y, \frac{3}{2}-z$]. As shown in Fig. 3*b*, the points of contact between layers involve methyl-C8—H···π interactions with the symmetry-related phenyl (C23–C28) ring, Table 2, resulting in a three-dimensional architecture.

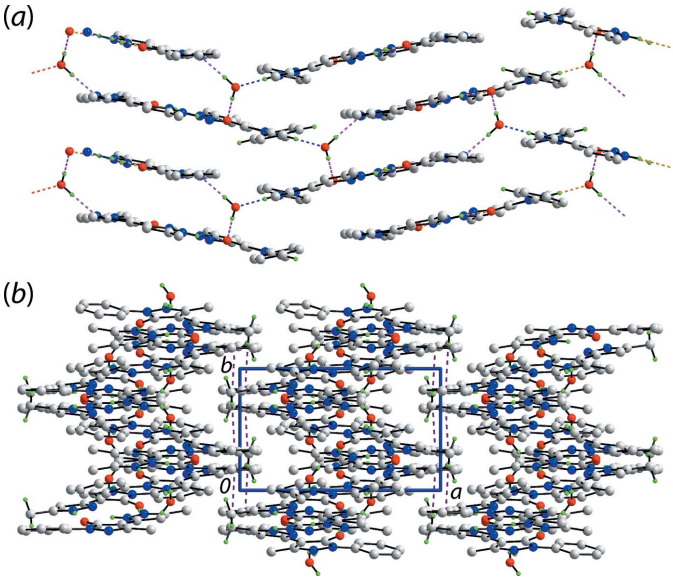

Figure 3
Supramolecular association in the crystal of (I): (*a*) a view of the supramolecular layer in the *bc* plane whereby the dimeric aggregates shown in Fig. 1 are connected by water-O1*W*···O1(carbonyl), water-O1*W*···N6(pyrazolide) (pink dashed lines) and pyrazolyl-N2—H···O1*W*(water) hydrogen bonds (blue dashed lines) and (*b*) a view of the unit-cell contents shown in projection down the *c* axis. The C—H···π interactions are shown as purple dashed lines. In both images, the non-participating and non-acidic H atoms are omitted.

4. Hirshfeld surface analysis

The Hirshfeld surface calculations for (I) were calculated employing *Crystal Explorer* (Turner *et al.*, 2017) and were conducted in accord with recent studies (Tan *et al.*, 2019) to investigate the influence of intermolecular interactions between the neutral and zwitterionic tautomers, along with the water molecule of crystallization, on the molecular packing.

The donors and acceptors of the hydrogen bonds summarized in Table 2 and discussed in the previous section are clearly evident as the broad and bright-red spots on the Hirshfeld surface mapped over d_{norm} for the neutral tautomer in Fig. 4*a* and *b* and for the zwitterionic tautomer in Fig. 4*c*. In addition to these, a short intramolecular H···H contact between symmetry-related pyrazolyl-H4*N* and H7*N* atoms (Table 3) is viewed as faint-red spots near these atoms on the d_{norm}-mapped Hirshfeld surfaces of the tautomers in Fig. 4*a* and *c*. It is clear from the views of the Hirshfeld surfaces mapped over the calculated electrostatic potential for neutral molecule in

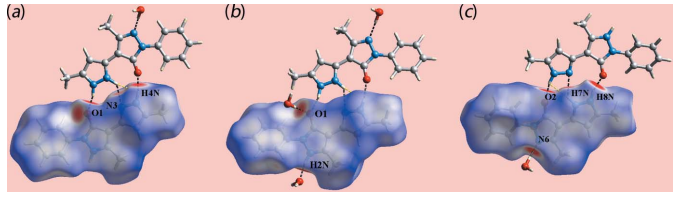

Figure 4
Views of the Hirshfeld surface for (I) mapped over d_{norm} in the range −0.527 to +1.288 arbitrary units for (*a*) and (*b*) the neutral tautomer and (*c*) in the range −0.527 to +1.367 arbitrary units for the zwitterion and a short intra-atomic H···H contact by a yellow dashed line.

Table 3
Summary of short interatomic contacts (Å) in (I).

Contact	Distance	Symmetry operation
H4*N*···H7*N*	2.05	*x*, *y*, *z*
H13···H18*A*	2.28	$x, \frac{1}{2}-y, \frac{1}{2}+z$
H14···H18*A*	2.05	$x, \frac{1}{2}-y, \frac{1}{2}+z$
C1···H1*W*	2.60	$1-x, 1-y, 1-z$
C10···H1*W*	2.81	$1-x, 1-y, 1-z$
C14···H18*A*	2.75	$x, \frac{1}{2}-y, \frac{1}{2}+z$
C28···H8*B*	2.75	$2-x, -y, 1-z$
N2···C14	3.238 (2)	$1-x, -\frac{1}{2}+y, \frac{3}{2}-z$
C2···C13	3.382 (3)	$1-x, -\frac{1}{2}+y, \frac{3}{2}-z$
C8···C22	3.317 (2)	$1+x, y, z$
C15···C22	3.352 (3)	$1-x, 1-y, 1-z$
C17···C21	3.391 (3)	$1-x, 1-y, 1-z$

Fig. 5*a* and *b*, and for the zwitterionic tautomer in Fig. 5*c* and *d*, that they have quite distinct charge distributions on their surfaces. The presence of non-protonated pyrazolyl-N3 and N6 atoms results in a pronounced electronegative regions adjacent to carbonyl-O1 atom in the neutral form and opposite to carbonyl-O2 atom in the zwitterion as shown by the intense-red regions in Fig. 5*a*–*d*; hence facilitating the charge-assisted hydrogen bonds with pyrazolyl-N7 and water-O1*W* atoms, respectively. The donors and acceptors of intermolecular water-O1*W*–-H···O1(carbonyl) and pyrazolyl-N2—H···O1*W*(water) are also viewed as blue and red regions in Fig. 5*e* and *f*.

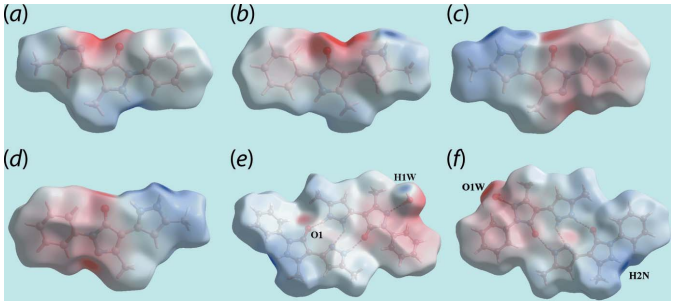

Figure 5
Views of Hirshfeld surface mapped over the calculated electrostatic potential for (*a*) and (*b*) the neutral tautomer in the range −0.157 to +0.225 atomic units (a.u.), (*c*) and (*d*) zwitterionic tautomer in the range −0.152 to +0.259 a.u., and (*e*) and (*f*) for the overall structure in the range −0.166 to +0.250 a.u.. The red and blue regions represent negative and positive electrostatic potentials, respectively.

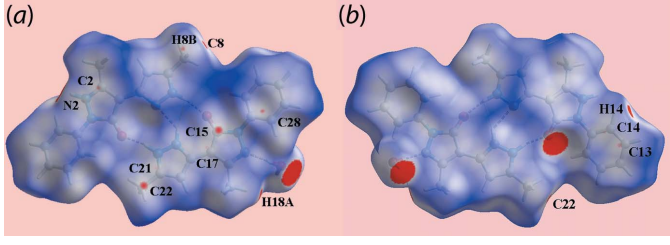

Figure 6
Views of Hirshfeld surfaces mapped over d_{norm} for the overall structure in the range −0.031 to +1.343 arbitrary units.

Table 4
Percentage contributions of interatomic contacts to the Hirshfeld surface for (I).

Contact	Percentage contribution		
	neutral tautomer	zwitterion	overall
H···H	49.8	52.4	52.4
O···H/H···O	11.1	9.4	8.8
N···H/H···N	8.2	14.0	9.1
C···H/H···C	21.5	15.1	19.9
C···C	5.2	5.9	5.9
C···N/N···C	4.9	3.1	3.7
C···O/O···C	0.2	0.1	0.2

Table 5
Geometric data (Å) for additional π–π interactions in the crystal of (I).

First ring	Second ring	Separation	Symmetry operation
Cg(N1,N2,C1–C3)	*Cg*(C9–C14)	3.5810 (9)	$1-x, \frac{1}{2}+y, \frac{3}{2}-z$
Cg(N5,N6,C15–C17)	*Cg*(N7,N8,C19–C21)	3.8064 (9)	$1-x, 1-y, 1-z$
Cg (N7,N8,C19–C21)	*Cg*(N7,N8,C19–C21)	3.6886 (10)	$1-x, -y, 1-z$

The short interatomic contacts characterizing weak intermolecular interactions in the crystal of (I) are viewed as characteristic red spots near the involved atoms on the Hirshfeld surface of the overall structure by modifying (making more sensitive) the d_{norm} range, see Fig. 6 and Table 3. The short intra- and inter-layer C···C contacts formed by the methyl-C22 atom with methyl-C8 and pyrazolyl-C15 atoms (Table 3) are viewed as small red spots near these atoms in Fig. 6*a*. The presence of faint-red spots near pyrazole-N2, C2, C17, C21 and phenyl-C13, C14 atoms in Fig. 6 represent their participation in short interatomic C···C and C···N contacts (Table 3) arising from π–π contacts between the N1-pyrazolyl and phenyl (C9–C14), and pyrazolyl-N5 and pyrazolyl-N7 rings (Table 5). In addition to this, the influence of short interatomic H···H and C···H/H···C contacts (Table 3) on the packing is also evident as the faint-red spots near methyl-H8*B* and phenyl-C28 atoms, and the spots near the methyl-H18*A* and phenyl-C14, H14 atoms in Fig. 6. The involvement of the methyl-H8*A* and H8*B* atoms as the donors and the phenyl (C23–C28) ring as the acceptor in the C—H···π contacts are also confirmed from the Hirshfeld surface mapped with the shape-index property through blue and red regions, respectively, in Fig. 7.

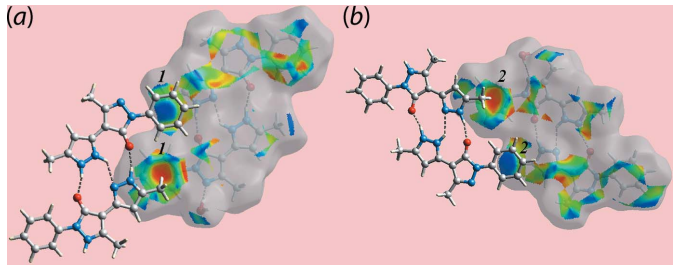

Figure 7
Views of Hirshfeld surfaces mapped with the shape-index property highlighting the donors (labelled '1′) and acceptors ('2′) of C—H···π contacts through blue and red regions, respectively.

The overall two dimensional fingerprint plot in Fig. 8*a* and those delineated into H···H, O···H/H···O, N···H/H···N and C···H/H···C, C···C and C···N/N···C contacts for the overall structure are illustrated in Fig. 8*b*–*g* and the percentage contributions from the different interatomic contacts to the Hirshfeld surfaces of the neutral tautomer, zwitterion and the overall structure are summarized in Table 4.

In the fingerprint plot delineated into H···H contacts, Fig. 8*b*, the short contact involving the methyl-H18*A* and phenyl-H14 atoms, Table 3, are viewed as the pair of two adjacent short peaks at $d_e + d_i$ ~2.1 Å while the points corresponding to the H13···H18*A* contact are merged within the plot. The involvement of the water molecule in the N—H···O hydrogen bond results in a pair of long spikes at $d_e + d_i$ ~1.8 Å in the fingerprint plot delineated into O···H/H···O contacts, Fig. 8*c*; these encompass the pair of spikes corresponding to the O—H···O hydrogen bond involving carbonyl-O1 atom. The percentage contribution from these contacts to the Hirshfeld surface of the overall structure is less than the individual tautomers (Table 4) as the atoms of the organic components comprising the asymmetric unit are self-associated by hydrogen bonds as well as participating in hydrogen bonding with the water molecule.

The fingerprint plot delineated into N···H/H···N contacts in Fig. 8*d* shows interatomic distances are at van der Waals separations or longer in the crystal. The significant 19.9% contribution from C···H/H···C contacts to the Hirshfeld surface of (I), Table 4, arises from a significant number of methyl-C—H···π(phenyl) interactions (Tables 2 and 3) and short phenyl-, pyrazolyl-C···H(water, methyl) contacts (Table 3). The presence of C—H···π interactions are viewed as the pair of characteristic wings in Fig. 8*e* with the shortest C···H contact represented as the pair of peaks at $d_e + d_i$ ~2.7 Å, Table 3. It is evident from the fingerprint plots delineated into C···C and C···N/N···C contacts in Fig. 8*f* and *g*, arise from the presence of inter-layer π–π contacts between pyrazolyl and phenyl rings whereas the other short C···C contacts summarized in Table 3 are intra-layer, *i.e.* methyl-C8···C22(methyl). The small contribution from C···O/O···C contacts appears to have a negligible effect on the molecular packing.

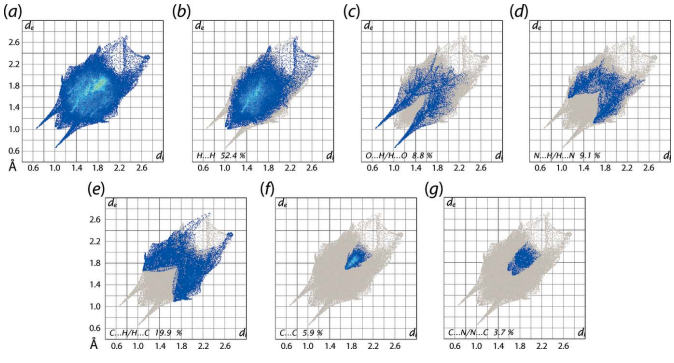

Figure 8
(*a*) The full two-dimensional fingerprint plot for (I) and (*b*)–(*f*) those delineated into H···H, O···H/H···O, N···H/H···N, C···H/H···C, C···C and C···N/N···C contacts, respectively.

Table 6
Experimental details.

Crystal data	
Chemical formula	$2C_{14}H_{14}N_4O{\cdot}H_2O$
M_r	526.60
Crystal system, space group	Monoclinic, $P2_1/c$
Temperature (K)	100
a, b, c (Å)	11.7007 (6), 7.0419 (3), 31.2567 (17)
β (°)	98.379 (5)
V (Å^3)	2547.9 (2)
Z	4
Radiation type	Mo $K\alpha$
μ (mm^{-1})	0.09
Crystal size (mm)	0.35 × 0.35 × 0.05
Data collection	
Diffractometer	Agilent SuperNova Dual diffractometer with an Atlas detector
Absorption correction	Multi-scan (*CrysAlis PRO*; Agilent, 2011)
T_{min}, T_{max}	0.968, 0.995
No. of measured, independent and observed [$I > 2\sigma(I)$] reflections	10823, 5838, 4411
R_{int}	0.031
(sin $\theta/\lambda)_{max}$ (Å^{-1})	0.651
Refinement	
$R[F^2 > 2\sigma(F^2)]$, $wR(F^2)$, S	0.052, 0.137, 1.06
No. of reflections	5838
No. of parameters	374
No. of restraints	6
H-atom treatment	H atoms treated by a mixture of independent and constrained refinement
$\Delta\rho_{max}$, $\Delta\rho_{min}$ (e Å^{-3})	0.27, −0.41

Computer programs: *CrysAlis PRO* (Agilent, 2011), *SHELXS97* (Sheldrick, 2015*a*), *SHELXL2018* (Sheldrick, 2015*b*), *ORTEP-3 for Windows* (Farrugia, 2012), *QMol*Gans & Shalloway (2001), *DIAMOND* (Brandenburg, 2006) and *publCIF* (Westrip, 2010).

5. Database survey

There are no direct precedents for the neutral molecule found in (I) in the crystallographic literature. Arguably, the most closely related species is the compound whereby the nitrogen-bound proton in the pendant five-membered ring has been substituted by a phenyl ring to give (II) – this structure has been reported three times [Bertolasi *et al.*, 1995 (ZILJIN); Kumar *et al.*, 1995 (ZILJIN01); Ghandour *et al.*, 2017 (ZILJIN02)]. Here, owing to the presence of the phenyl ring, there is a significant twist between the five-membered rings as seen in the $C_{carbonyl}$—C—C—$N_{external\ ring}$ torsion angle of 57.1 (3)°. In two other derivatives, a similar situation pertains. In the derivative where the original phenyl ring of the neutral molecule in (I) is substituted with a benzenesulfonamide group (EXIJEB; Asiri *et al.*, 2011), the equivalent torsion angle is 132.9 (2)°. Finally, when both phenyl groups of (II) are substituted with 4-chlorobenzene rings (KUZPIF; Rabnawaz *et al.*, 2010), $C_{carbonyl}$—C—C—$N_{external\ ring}$ torsion angles of −57 (1) and 56 (1)° are found for the two crystallographically independent molecules comprising the asymmetric unit.

6. Synthesis and crystallization

4-Acetoacetyl-3-methyl-1-phenyl-2-pyrazolin-5-one 1 (2.5 g, 10 mmol) and hydrazin hydrazine (1 ml) were refluxed in a mixture of ethanol (50 ml) and acetic acid (50 ml) for 2 h. The reaction mixture was allowed to stand at room temperature. The precipitate was filtered and recrystallized from ethanol solution as fine needles, M.p. 409–410 K. Yield: 70%.

7. Refinement details

Crystal data, data collection and structure refinement details are summarized in Table 6. The carbon-bound H atoms were placed in calculated positions (C—H = 0.95–0.98 Å) and were included in the refinement in the riding-model approximation, with U_{iso}(H) set to 1.2–1.5U_{eq}(C). The O- and N-bound H atoms were refined with distance restraints of 0.84±0.01 and 0.86±0.01 Å, respectively, and with U_{iso}(H) = 1.5U_{eq}(O) and 1.2U_{eq}(N).

Acknowledgements

The University of Malaya's X-ray crystallography laboratory is thanked for the intensity data.

Funding information

This research was funded by the Deanship of Scientific Research (DSR) at King Abdulaziz University, Jeddah, under grant No. RG-03–102-428.

References

Agilent (2011). *CrysAlis PRO*. Agilent Technologies, Yarnton, England.
Asiri, A. M., Al-Youbi, A. O., Faidallah, H. M., Alamry, K. A. & Ng, S. W. (2011). *Acta Cryst.* E**67**, o2474.
Badawey, E. A. M. & El-Ashmawey, I. M. (1998). *Eur. J. Med. Chem.* **33**, 349–361.
Bertolasi, V., Gilli, P., Ferretti, V. & Gilli, G. (1995). *Acta Cryst.* B**51**, 1004–1015.
Brandenburg, K. (2006). *DIAMOND*. Crystal Impact GbR, Bonn, Germany.
Das, N., Verma, A., Shrivastava, P. K. & Shrivastava, S. K. (2008). *Indian J. Chem. Sect. B*, **47**, 1555–1558.
Farrugia, L. J. (2012). *J. Appl. Cryst.* **45**, 849–854.
Gans, J. & Shalloway, D. (2001). *J. Mol. Graph. Model.* **19**, 557–559.
Ghandour, I., Mague, J. T., Bouayad, A., Chakroune, S., Essassi, E. M. & Kandri Rodi, Y. (2017). *IUCrData*, **2**, x170853.
Higashi, Y., Jitsuiki, D., Chayama, K. & Yoshizumi, M. (2006). *Recent. Pat. Cardiovasc. Drug. Discov.* **1**, 85–93.
Kumar, D., Singh, S. P., Martínez, A., Fruchier, A., Elguero, J., Martínez-Ripoll, M., Carrió, J. S. & Virgili, A. (1995). *Tetrahedron*, **51**, 4891–4906.
Pizzala, H., Carles, M., Stone, W. E. E. & Thevand, A. (2000). *J. Mol. Struct.* **526**, 261–268.
Rabnawaz, M., Raza Shah, M. & Ng, S. W. (2010). *Acta Cryst.* E**66**, o2569.
Rubčić, M., Užarević, K., Halasz, I., Bregović, N., Mališ, M., Đilović, I., Kokan, Z., Stein, R. S., Dinnebier, R. E. & Tomišić, V. (2012). *Chem. Eur. J.* **18**, 5620–5631.
Sahu, S. K., Azam, A. M., Banerjee, M., Choudhary, P., Sutradhar, S., Panda, P. K. & Misra, P. K. (2007). *J. Indian Chem. Soc.* **84**, 1011–1015.
Sharma, B. D. & McConnell, J. F. (1965). *Acta Cryst.* **19**, 797–806.
Sheldrick, G. M. (2015*a*). *Acta Cryst.* A**71**, 3–8.
Sheldrick, G. M. (2015*b*). *Acta Cryst.* C**71**, 3–8.
Singh, D. & Singh, D. (1991). *J. Indian Chem. Soc.* **68**, 165–167.
Steiner, T. & Koellner, G. (1997). *Chem. Commun.* pp. 1207–1208.
Tan, S. L., Jotani, M. M. & Tiekink, E. R. T. (2019). *Acta Cryst.* E**75**, 308–318.
Turner, M. J., Mckinnon, J. J., Wolff, S. K., Grimwood, D. J., Spackman, P. R., Jayatilaka, D. & Spackman, M. A. (2017). Crystal Explorer v17. The University of Western Australia.
Westrip, S. P. (2010). *J. Appl. Cryst.* **43**, 920–925.

supporting information

Acta Cryst. (2019). E**75**, 565-570 [https://doi.org/10.1107/S2056989019004389]

Co-crystallization of a neutral molecule and its zwitterionic tautomer: structure and Hirshfeld surface analysis of 5-methyl-4-(5-methyl-1*H*-pyrazol-3-yl)-2-phenyl-2,3-dihydro-1*H*-pyrazol-3-one 5-methyl-4-(5-methyl-1*H*-pyrazol-2-ium-3-yl)-3-oxo-2-phenyl-2,3-dihydro-1*H*-pyrazol-1-ide monohydrate

Abdullah M. Asiri, Khalid A. H. Alzahrani, Hassan M. Faidallah, Khalid A. Alamry, Mukesh M. Jotani and Edward R. T. Tiekink

Computing details

Data collection: *CrysAlis PRO* (Agilent, 2011); cell refinement: *CrysAlis PRO* (Agilent, 2011); data reduction: *CrysAlis PRO* (Agilent, 2011); program(s) used to solve structure: *SHELXS97* (Sheldrick, 2015*a*); program(s) used to refine structure: *SHELXL2018* (Sheldrick, 2015*b*); molecular graphics: *ORTEP-3 for Windows* (Farrugia, 2012), *QMol*Gans & Shalloway (2001) and *DIAMOND* (Brandenburg, 2006); software used to prepare material for publication: *publCIF* (Westrip, 2010).

5-Methyl-4-(5-methyl-1*H*-pyrazol-3-yl)-2-phenyl-2,3-dihydro-1*H*-pyrazol-3-one 5-methyl-4-(5-methyl-1*H*-pyrazol-2-ium-3-yl)-3-oxo-2-phenyl-2,3-dihydro-1*H*-pyrazol-1-ide monohydrate

Crystal data

$2C_{14}H_{14}N_4O{\cdot}H_2O$
$M_r = 526.60$
Monoclinic, $P2_1/c$
$a = 11.7007$ (6) Å
$b = 7.0419$ (3) Å
$c = 31.2567$ (17) Å
$\beta = 98.379$ (5)°
$V = 2547.9$ (2) Å^3
$Z = 4$
$F(000) = 1112$
$D_x = 1.373$ Mg m^{-3}
Mo $K\alpha$ radiation, $\lambda = 0.71073$ Å
Cell parameters from 3750 reflections
$\theta = 2.3$–$27.5°$
$\mu = 0.09$ mm^{-1}
$T = 100$ K
Plate, colourless
0.35 × 0.35 × 0.05 mm

Data collection

Agilent SuperNova Dual diffractometer with an Atlas detector
Radiation source: SuperNova (Mo) X-ray Source
Mirror monochromator
Detector resolution: 10.4041 pixels mm^{-1}
ω scan
Absorption correction: multi-scan (CrysAlis PRO; Agilent, 2011)
$T_{min} = 0.968$, $T_{max} = 0.995$
10823 measured reflections
5838 independent reflections
4411 reflections with $I > 2\sigma(I)$
$R_{int} = 0.031$
$\theta_{max} = 27.6°$, $\theta_{min} = 2.4°$
$h = -15\rightarrow9$
$k = -5\rightarrow9$
$l = -40\rightarrow39$

Refinement

Refinement on F^2
Least-squares matrix: full
$R[F^2 > 2\sigma(F^2)] = 0.052$
$wR(F^2) = 0.137$
$S = 1.06$
5838 reflections
374 parameters
6 restraints

Primary atom site location: structure-invariant direct methods
Hydrogen site location: mixed
H atoms treated by a mixture of independent and constrained refinement
$w = 1/[\sigma^2(F_o^2) + (0.0593P)^2 + 0.7451P]$ where $P = (F_o^2 + 2F_c^2)/3$
$(\Delta/\sigma)_{max} = 0.001$
$\Delta\rho_{max} = 0.27$ e Å^{-3}
$\Delta\rho_{min} = -0.40$ e Å^{-3}

Special details

Geometry. All esds (except the esd in the dihedral angle between two l.s. planes) are estimated using the full covariance matrix. The cell esds are taken into account individually in the estimation of esds in distances, angles and torsion angles; correlations between esds in cell parameters are only used when they are defined by crystal symmetry. An approximate (isotropic) treatment of cell esds is used for estimating esds involving l.s. planes.

Fractional atomic coordinates and isotropic or equivalent isotropic displacement parameters (Å²)

	x	*y*	*z*	U_{iso}*/U_{eq}
O1	0.50164 (10)	0.12787 (17)	0.64929 (4)	0.0181 (3)
N1	0.53780 (11)	0.0341 (2)	0.72110 (5)	0.0153 (3)
N2	0.63356 (12)	0.0066 (2)	0.75165 (5)	0.0160 (3)
N3	0.73563 (12)	0.1334 (2)	0.61575 (5)	0.0210 (3)
H2N	0.6292 (16)	−0.025 (3)	0.7792 (4)	0.025*
N4	0.83286 (12)	0.1666 (2)	0.59759 (5)	0.0208 (3)
H4N	0.8238 (17)	0.188 (3)	0.5695 (3)	0.025*
C1	0.57339 (14)	0.0824 (2)	0.68201 (5)	0.0148 (3)
C2	0.72834 (14)	0.0263 (2)	0.73272 (6)	0.0159 (4)
C3	0.69669 (14)	0.0740 (2)	0.68942 (5)	0.0150 (3)
C4	0.84351 (14)	−0.0047 (3)	0.75912 (6)	0.0194 (4)
H4A	0.833118	−0.055901	0.787460	0.029*
H4B	0.885122	0.116239	0.762975	0.029*
H4C	0.888010	−0.095029	0.744297	0.029*
C5	0.77502 (14)	0.1141 (2)	0.65819 (6)	0.0150 (3)
C6	0.89639 (14)	0.1367 (2)	0.66601 (6)	0.0172 (4)
H6	0.944899	0.130460	0.693134	0.021*
C7	0.92969 (14)	0.1697 (2)	0.62624 (6)	0.0171 (4)
C8	1.04501 (14)	0.1965 (3)	0.61202 (6)	0.0212 (4)
H8A	1.039270	0.293826	0.589397	0.032*
H8B	1.070308	0.076438	0.600611	0.032*
H8C	1.101164	0.236834	0.636718	0.032*
C9	0.42443 (14)	0.0244 (2)	0.73226 (6)	0.0151 (3)
C10	0.33184 (14)	−0.0258 (2)	0.70096 (6)	0.0177 (4)
H10	0.344090	−0.057124	0.672419	0.021*
C11	0.22132 (14)	−0.0291 (2)	0.71232 (6)	0.0196 (4)
H11	0.157180	−0.057578	0.690979	0.024*
C12	0.20340 (14)	0.0087 (2)	0.75446 (6)	0.0196 (4)
H12	0.127628	0.003740	0.761951	0.024*

C13	0.29632 (14)	0.0537 (3)	0.78551 (6)	0.0193 (4)
H13	0.284374	0.077360	0.814448	0.023*
C14	0.40700 (14)	0.0643 (2)	0.77450 (6)	0.0178 (4)
H14	0.470414	0.098477	0.795649	0.021*
O2	0.77522 (10)	0.25890 (19)	0.51120 (4)	0.0248 (3)
N5	0.74784 (12)	0.3174 (2)	0.43598 (5)	0.0155 (3)
N6	0.65481 (12)	0.3330 (2)	0.40247 (5)	0.0173 (3)
N7	0.56152 (12)	0.2282 (2)	0.53983 (5)	0.0178 (3)
H7N	0.6363 (9)	0.222 (3)	0.5506 (6)	0.021*
N8	0.47846 (12)	0.1938 (2)	0.56454 (5)	0.0177 (3)
H8N	0.4983 (16)	0.166 (3)	0.5926 (3)	0.021*
C15	0.71023 (14)	0.2837 (2)	0.47567 (6)	0.0165 (4)
C16	0.56071 (14)	0.3123 (2)	0.42123 (6)	0.0163 (4)
C17	0.58821 (14)	0.2820 (2)	0.46598 (5)	0.0153 (3)
C18	0.44402 (15)	0.3236 (3)	0.39471 (6)	0.0237 (4)
H18A	0.452353	0.350197	0.364543	0.036*
H18B	0.399461	0.425608	0.405806	0.036*
H18C	0.403635	0.202539	0.396371	0.036*
C19	0.51492 (14)	0.2495 (2)	0.49802 (5)	0.0151 (3)
C20	0.39512 (14)	0.2301 (2)	0.49695 (6)	0.0169 (4)
H20	0.337894	0.239186	0.472140	0.020*
C21	0.37622 (14)	0.1949 (2)	0.53908 (6)	0.0166 (4)
C22	0.26704 (15)	0.1657 (3)	0.55739 (6)	0.0220 (4)
H22A	0.282458	0.086869	0.583433	0.033*
H22B	0.210356	0.102077	0.535950	0.033*
H22C	0.236420	0.288951	0.564862	0.033*
C23	0.86164 (14)	0.3190 (2)	0.42595 (6)	0.0158 (4)
C24	0.95656 (15)	0.3283 (3)	0.45857 (6)	0.0241 (4)
H24	0.945472	0.331769	0.488071	0.029*
C25	1.06731 (16)	0.3324 (3)	0.44760 (7)	0.0287 (5)
H25	1.131685	0.340211	0.469881	0.034*
C26	1.08599 (15)	0.3254 (3)	0.40489 (6)	0.0248 (4)
H26	1.162274	0.326228	0.397846	0.030*
C27	0.99162 (15)	0.3172 (3)	0.37267 (6)	0.0207 (4)
H27	1.003385	0.313770	0.343246	0.025*
C28	0.87980 (14)	0.3139 (2)	0.38275 (6)	0.0180 (4)
H28	0.815760	0.308261	0.360297	0.022*
O1W	0.65340 (10)	0.59378 (18)	0.33486 (4)	0.0195 (3)
H1W	0.6112 (15)	0.686 (2)	0.3408 (7)	0.029*
H2W	0.6537 (17)	0.512 (2)	0.3552 (5)	0.029*

Atomic displacement parameters (Å²)

	U^{11}	U^{22}	U^{33}	U^{12}	U^{13}	U^{23}
O1	0.0169 (6)	0.0268 (7)	0.0107 (6)	0.0025 (5)	0.0026 (5)	0.0029 (5)
N1	0.0152 (7)	0.0215 (7)	0.0092 (7)	−0.0003 (6)	0.0020 (5)	0.0006 (6)
N2	0.0162 (7)	0.0228 (7)	0.0090 (7)	−0.0007 (6)	0.0017 (6)	0.0018 (6)
N3	0.0169 (7)	0.0347 (9)	0.0125 (8)	−0.0008 (6)	0.0064 (6)	0.0028 (7)

N4	0.0173 (7)	0.0344 (9)	0.0117 (8)	0.0005 (6)	0.0052 (6)	0.0054 (7)
C1	0.0185 (8)	0.0150 (8)	0.0116 (8)	−0.0001 (6)	0.0042 (7)	−0.0001 (7)
C2	0.0183 (8)	0.0167 (8)	0.0136 (9)	−0.0010 (6)	0.0047 (7)	0.0004 (7)
C3	0.0164 (8)	0.0174 (8)	0.0114 (8)	0.0005 (6)	0.0031 (6)	0.0009 (7)
C4	0.0182 (8)	0.0248 (9)	0.0150 (9)	−0.0011 (7)	0.0016 (7)	0.0021 (7)
C5	0.0168 (8)	0.0161 (8)	0.0124 (8)	−0.0002 (6)	0.0035 (7)	−0.0008 (7)
C6	0.0158 (8)	0.0238 (9)	0.0122 (9)	0.0001 (7)	0.0023 (7)	0.0012 (7)
C7	0.0180 (8)	0.0185 (8)	0.0158 (9)	0.0023 (7)	0.0056 (7)	0.0025 (7)
C8	0.0186 (9)	0.0255 (9)	0.0215 (10)	0.0017 (7)	0.0092 (7)	0.0046 (8)
C9	0.0162 (8)	0.0160 (8)	0.0141 (9)	0.0008 (6)	0.0054 (7)	0.0038 (7)
C10	0.0213 (8)	0.0199 (8)	0.0124 (9)	−0.0004 (7)	0.0038 (7)	0.0014 (7)
C11	0.0188 (8)	0.0212 (9)	0.0180 (9)	−0.0016 (7)	0.0000 (7)	0.0011 (7)
C12	0.0170 (8)	0.0224 (9)	0.0206 (10)	−0.0006 (7)	0.0068 (7)	0.0012 (8)
C13	0.0211 (9)	0.0255 (9)	0.0126 (9)	0.0021 (7)	0.0065 (7)	0.0005 (7)
C14	0.0177 (8)	0.0234 (9)	0.0123 (9)	0.0007 (7)	0.0023 (7)	0.0011 (7)
O2	0.0178 (6)	0.0448 (8)	0.0114 (6)	−0.0039 (6)	0.0005 (5)	0.0048 (6)
N5	0.0149 (7)	0.0214 (7)	0.0103 (7)	0.0001 (6)	0.0025 (5)	0.0021 (6)
N6	0.0153 (7)	0.0249 (8)	0.0111 (7)	0.0002 (6)	0.0003 (6)	0.0011 (6)
N7	0.0153 (7)	0.0268 (8)	0.0118 (7)	−0.0001 (6)	0.0038 (6)	0.0005 (6)
N8	0.0192 (7)	0.0247 (8)	0.0101 (7)	−0.0011 (6)	0.0050 (6)	0.0012 (6)
C15	0.0185 (8)	0.0197 (8)	0.0116 (8)	−0.0021 (7)	0.0031 (7)	−0.0008 (7)
C16	0.0176 (8)	0.0197 (8)	0.0122 (9)	0.0002 (7)	0.0043 (7)	0.0011 (7)
C17	0.0167 (8)	0.0182 (8)	0.0115 (8)	−0.0014 (6)	0.0036 (6)	−0.0008 (7)
C18	0.0165 (8)	0.0415 (11)	0.0132 (9)	−0.0004 (8)	0.0023 (7)	0.0054 (8)
C19	0.0182 (8)	0.0166 (8)	0.0109 (8)	−0.0002 (6)	0.0032 (6)	−0.0012 (7)
C20	0.0161 (8)	0.0222 (9)	0.0124 (9)	−0.0011 (7)	0.0027 (6)	−0.0001 (7)
C21	0.0181 (8)	0.0169 (8)	0.0155 (9)	−0.0002 (6)	0.0046 (7)	0.0006 (7)
C22	0.0220 (9)	0.0267 (9)	0.0190 (10)	−0.0002 (7)	0.0094 (7)	0.0006 (8)
C23	0.0156 (8)	0.0176 (8)	0.0151 (9)	0.0000 (6)	0.0053 (7)	0.0016 (7)
C24	0.0199 (9)	0.0377 (11)	0.0148 (9)	−0.0012 (8)	0.0033 (7)	0.0013 (8)
C25	0.0189 (9)	0.0462 (12)	0.0206 (10)	−0.0001 (8)	0.0014 (8)	0.0044 (9)
C26	0.0174 (9)	0.0330 (10)	0.0257 (11)	0.0013 (8)	0.0085 (8)	0.0033 (8)
C27	0.0214 (9)	0.0252 (9)	0.0172 (9)	0.0017 (7)	0.0090 (7)	0.0000 (7)
C28	0.0180 (8)	0.0224 (9)	0.0136 (9)	0.0002 (7)	0.0027 (7)	0.0000 (7)
O1W	0.0239 (7)	0.0224 (6)	0.0131 (7)	0.0050 (5)	0.0058 (5)	0.0022 (5)

Geometric parameters (Å, º)

O1—C1	1.266 (2)	N5—C15	1.396 (2)
N1—N2	1.3759 (19)	N5—N6	1.4006 (19)
N1—C1	1.389 (2)	N5—C23	1.412 (2)
N1—C9	1.422 (2)	N6—C16	1.329 (2)
N2—C2	1.338 (2)	N7—N8	1.3486 (19)
N2—H2N	0.898 (9)	N7—C19	1.349 (2)
N3—C5	1.346 (2)	N7—H7N	0.892 (9)
N3—N4	1.3636 (19)	N8—C21	1.337 (2)
N4—C7	1.338 (2)	N8—H8N	0.894 (9)
N4—H4N	0.882 (9)	C15—C17	1.416 (2)

C1—C3	1.429 (2)	C16—C17	1.405 (2)
C2—C3	1.391 (2)	C16—C18	1.493 (2)
C2—C4	1.490 (2)	C17—C19	1.429 (2)
C3—C5	1.461 (2)	C18—H18A	0.9800
C4—H4A	0.9800	C18—H18B	0.9800
C4—H4B	0.9800	C18—H18C	0.9800
C4—H4C	0.9800	C19—C20	1.404 (2)
C5—C6	1.414 (2)	C20—C21	1.389 (2)
C6—C7	1.375 (2)	C20—H20	0.9500
C6—H6	0.9500	C21—C22	1.488 (2)
C7—C8	1.493 (2)	C22—H22A	0.9800
C8—H8A	0.9800	C22—H22B	0.9800
C8—H8B	0.9800	C22—H22C	0.9800
C8—H8C	0.9800	C23—C24	1.396 (2)
C9—C14	1.394 (2)	C23—C28	1.397 (2)
C9—C10	1.395 (2)	C24—C25	1.388 (2)
C10—C11	1.390 (2)	C24—H24	0.9500
C10—H10	0.9500	C25—C26	1.385 (3)
C11—C12	1.389 (2)	C25—H25	0.9500
C11—H11	0.9500	C26—C27	1.383 (3)
C12—C13	1.384 (2)	C26—H26	0.9500
C12—H12	0.9500	C27—C28	1.390 (2)
C13—C14	1.390 (2)	C27—H27	0.9500
C13—H13	0.9500	C28—H28	0.9500
C14—H14	0.9500	O1W—H1W	0.851 (9)
O2—C15	1.263 (2)	O1W—H2W	0.858 (9)

N2—N1—C1	109.07 (13)	C15—N5—C23	128.95 (15)
N2—N1—C9	121.16 (14)	N6—N5—C23	119.25 (14)
C1—N1—C9	129.62 (14)	C16—N6—N5	105.37 (13)
C2—N2—N1	108.78 (14)	N8—N7—C19	110.58 (14)
C2—N2—H2N	128.0 (12)	N8—N7—H7N	121.6 (13)
N1—N2—H2N	123.1 (12)	C19—N7—H7N	127.4 (13)
C5—N3—N4	103.94 (14)	C21—N8—N7	108.36 (14)
C7—N4—N3	113.60 (14)	C21—N8—H8N	131.8 (13)
C7—N4—H4N	129.1 (13)	N7—N8—H8N	119.6 (13)
N3—N4—H4N	117.2 (13)	O2—C15—N5	125.28 (15)
O1—C1—N1	121.59 (14)	O2—C15—C17	130.23 (16)
O1—C1—C3	132.57 (15)	N5—C15—C17	104.49 (14)
N1—C1—C3	105.80 (14)	N6—C16—C17	111.82 (15)
N2—C2—C3	109.58 (15)	N6—C16—C18	119.93 (15)
N2—C2—C4	118.72 (15)	C17—C16—C18	128.26 (15)
C3—C2—C4	131.70 (15)	C16—C17—C15	106.80 (14)
C2—C3—C1	106.69 (14)	C16—C17—C19	130.42 (16)
C2—C3—C5	126.36 (15)	C15—C17—C19	122.76 (15)
C1—C3—C5	126.92 (15)	C16—C18—H18A	109.5
C2—C4—H4A	109.5	C16—C18—H18B	109.5
C2—C4—H4B	109.5	H18A—C18—H18B	109.5

H4A—C4—H4B	109.5	C16—C18—H18C	109.5
C2—C4—H4C	109.5	H18A—C18—H18C	109.5
H4A—C4—H4C	109.5	H18B—C18—H18C	109.5
H4B—C4—H4C	109.5	N7—C19—C20	105.87 (15)
N3—C5—C6	110.48 (15)	N7—C19—C17	119.85 (15)
N3—C5—C3	121.32 (15)	C20—C19—C17	134.28 (16)
C6—C5—C3	128.19 (16)	C21—C20—C19	106.93 (15)
C7—C6—C5	105.80 (15)	C21—C20—H20	126.5
C7—C6—H6	127.1	C19—C20—H20	126.5
C5—C6—H6	127.1	N8—C21—C20	108.26 (14)
N4—C7—C6	106.17 (15)	N8—C21—C22	120.92 (16)
N4—C7—C8	121.10 (16)	C20—C21—C22	130.81 (16)
C6—C7—C8	132.67 (16)	C21—C22—H22A	109.5
C7—C8—H8A	109.5	C21—C22—H22B	109.5
C7—C8—H8B	109.5	H22A—C22—H22B	109.5
H8A—C8—H8B	109.5	C21—C22—H22C	109.5
C7—C8—H8C	109.5	H22A—C22—H22C	109.5
H8A—C8—H8C	109.5	H22B—C22—H22C	109.5
H8B—C8—H8C	109.5	C24—C23—C28	119.36 (15)
C14—C9—C10	120.62 (15)	C24—C23—N5	120.93 (16)
C14—C9—N1	119.57 (15)	C28—C23—N5	119.70 (15)
C10—C9—N1	119.81 (15)	C25—C24—C23	119.51 (18)
C11—C10—C9	118.77 (16)	C25—C24—H24	120.2
C11—C10—H10	120.6	C23—C24—H24	120.2
C9—C10—H10	120.6	C26—C25—C24	121.44 (18)
C12—C11—C10	120.89 (16)	C26—C25—H25	119.3
C12—C11—H11	119.6	C24—C25—H25	119.3
C10—C11—H11	119.6	C27—C26—C25	118.82 (16)
C13—C12—C11	119.79 (16)	C27—C26—H26	120.6
C13—C12—H12	120.1	C25—C26—H26	120.6
C11—C12—H12	120.1	C26—C27—C28	120.91 (17)
C12—C13—C14	120.26 (16)	C26—C27—H27	119.5
C12—C13—H13	119.9	C28—C27—H27	119.5
C14—C13—H13	119.9	C27—C28—C23	119.95 (16)
C13—C14—C9	119.61 (16)	C27—C28—H28	120.0
C13—C14—H14	120.2	C23—C28—H28	120.0
C9—C14—H14	120.2	H1W—O1W—H2W	107.0 (19)
C15—N5—N6	111.51 (13)		

C1—N1—N2—C2	−3.11 (18)	C15—N5—N6—C16	0.98 (18)
C9—N1—N2—C2	−179.05 (15)	C23—N5—N6—C16	175.29 (15)
C5—N3—N4—C7	−0.2 (2)	C19—N7—N8—C21	−0.87 (19)
N2—N1—C1—O1	−175.10 (14)	N6—N5—C15—O2	178.15 (16)
C9—N1—C1—O1	0.4 (3)	C23—N5—C15—O2	4.5 (3)
N2—N1—C1—C3	2.85 (17)	N6—N5—C15—C17	−1.05 (18)
C9—N1—C1—C3	178.34 (16)	C23—N5—C15—C17	−174.67 (16)
N1—N2—C2—C3	2.06 (19)	N5—N6—C16—C17	−0.50 (19)
N1—N2—C2—C4	−177.61 (14)	N5—N6—C16—C18	179.24 (15)

N2—C2—C3—C1	−0.27 (19)	N6—C16—C17—C15	−0.1 (2)
C4—C2—C3—C1	179.35 (17)	C18—C16—C17—C15	−179.85 (17)
N2—C2—C3—C5	177.71 (15)	N6—C16—C17—C19	−178.60 (17)
C4—C2—C3—C5	−2.7 (3)	C18—C16—C17—C19	1.7 (3)
O1—C1—C3—C2	176.04 (17)	O2—C15—C17—C16	−178.44 (18)
N1—C1—C3—C2	−1.59 (18)	N5—C15—C17—C16	0.70 (18)
O1—C1—C3—C5	−1.9 (3)	O2—C15—C17—C19	0.2 (3)
N1—C1—C3—C5	−179.55 (15)	N5—C15—C17—C19	179.32 (15)
N4—N3—C5—C6	0.35 (19)	N8—N7—C19—C20	1.01 (19)
N4—N3—C5—C3	−179.20 (15)	N8—N7—C19—C17	−178.27 (15)
C2—C3—C5—N3	170.80 (16)	C16—C17—C19—N7	−178.44 (17)
C1—C3—C5—N3	−11.6 (3)	C15—C17—C19—N7	3.3 (3)
C2—C3—C5—C6	−8.7 (3)	C16—C17—C19—C20	2.5 (3)
C1—C3—C5—C6	168.93 (17)	C15—C17—C19—C20	−175.72 (18)
N3—C5—C6—C7	−0.34 (19)	N7—C19—C20—C21	−0.76 (19)
C3—C5—C6—C7	179.16 (16)	C17—C19—C20—C21	178.35 (18)
N3—N4—C7—C6	0.0 (2)	N7—N8—C21—C20	0.35 (19)
N3—N4—C7—C8	177.54 (15)	N7—N8—C21—C22	−178.43 (15)
C5—C6—C7—N4	0.18 (19)	C19—C20—C21—N8	0.26 (19)
C5—C6—C7—C8	−176.92 (18)	C19—C20—C21—C22	178.88 (18)
N2—N1—C9—C14	26.2 (2)	C15—N5—C23—C24	−15.1 (3)
C1—N1—C9—C14	−148.83 (17)	N6—N5—C23—C24	171.73 (15)
N2—N1—C9—C10	−153.49 (15)	C15—N5—C23—C28	165.82 (16)
C1—N1—C9—C10	31.5 (3)	N6—N5—C23—C28	−7.4 (2)
C14—C9—C10—C11	2.1 (3)	C28—C23—C24—C25	0.0 (3)
N1—C9—C10—C11	−178.19 (15)	N5—C23—C24—C25	−179.08 (17)
C9—C10—C11—C12	−2.8 (3)	C23—C24—C25—C26	−0.7 (3)
C10—C11—C12—C13	1.2 (3)	C24—C25—C26—C27	1.0 (3)
C11—C12—C13—C14	1.1 (3)	C25—C26—C27—C28	−0.7 (3)
C12—C13—C14—C9	−1.7 (3)	C26—C27—C28—C23	0.0 (3)
C10—C9—C14—C13	0.1 (3)	C24—C23—C28—C27	0.3 (3)
N1—C9—C14—C13	−179.61 (16)	N5—C23—C28—C27	179.44 (16)

Hydrogen-bond geometry (Å, º)

*Cg*1 is the centroid of the (C23–C28) ring.

D—H···*A*	*D*—H	H···*A*	*D*···*A*	*D*—H···*A*
N2—H2*N*···O1*W*^{i}	0.90 (1)	1.79 (1)	2.673 (2)	168 (2)
N4—H4*N*···O2	0.88 (1)	1.90 (1)	2.764 (2)	168 (2)
N7—H7*N*···N3	0.89 (1)	2.28 (2)	2.970 (2)	134 (1)
N8—H8*N*···O1	0.90 (1)	1.79 (1)	2.664 (2)	166 (2)
O1*W*—H1*W*···O1^{ii}	0.85 (2)	1.92 (2)	2.7641 (17)	172 (2)
O1*W*—H2*W*···N6	0.86 (2)	1.94 (2)	2.7979 (19)	178 (2)
C8—H8*A*···*Cg*1^{iii}	0.98	2.71	3.492 (2)	137
C8—H8*B*···*Cg*1^{iv}	0.98	2.89	3.755 (2)	148

Symmetry codes: (i) *x*, −*y*+1/2, *z*+1/2; (ii) −*x*+1, −*y*+1, −*z*+1; (iii) −*x*+2, −*y*+1, −*z*+1; (iv) −*x*+2, −*y*, −*z*+1.